



AFRL-OSR-VA-TR-2013-0404

Atmospheric polarization imaging with variable aerosols, clouds, and surface albedo.

**Dr. Joseph
Shaw
Montana State University**

**JULY 2013
Final Report**

DISTRIBUTION A: Approved for public release.

**AIR FORCE RESEARCH LABORATORY
AF OFFICE OF SCIENTIFIC RESEARCH (AFOSR)
ARLINGTON, VIRGINIA 22203
AIR FORCE MATERIEL COMMAND**

REPORT DOCUMENTATION PAGE				Form Approved OMB No. 0704-0188	
Public reporting burden for this collection of information is estimated to average 1 hour per response, including the time for reviewing instructions, searching existing data sources, gathering and maintaining the data needed, and completing and reviewing this collection of information. Send comments regarding this burden estimate or any other aspect of this collection of information, including suggestions for reducing this burden to Department of Defense, Washington Headquarters Services, Directorate for Information Operations and Reports (0704-0188), 1215 Jefferson Davis Highway, Suite 1204, Arlington, VA 22202-4302. Respondents should be aware that notwithstanding any other provision of law, no person shall be subject to any penalty for failing to comply with a collection of information if it does not display a currently valid OMB control number. PLEASE DO NOT RETURN YOUR FORM TO THE ABOVE ADDRESS.					
1. REPORT DATE (DD-MM-YYYY) 7-15-2013		2. REPORT TYPE Final Technical Report		3. DATES COVERED (From - To) April 2010 - April 2013	
4. TITLE AND SUBTITLE Atmospheric polarization imaging with variable aerosols, Clouds, and surface albedo.				5a. CONTRACT NUMBER	
				5b. GRANT NUMBER FA9550-10-1-0115	
				5c. PROGRAM ELEMENT NUMBER	
6. AUTHOR(S) Dr. Joseph A. Shaw				5d. PROJECT NUMBER	
				5e. TASK NUMBER	
				5f. WORK UNIT NUMBER	
7. PERFORMING ORGANIZATION NAME(S) AND ADDRESS(ES) Montana State University Office of Sponsored Programs 307 Montana Hall Bozeman, MT 59717-0001				8. PERFORMING ORGANIZATION REPORT NUMBER	
9. SPONSORING / MONITORING AGENCY NAME(S) AND ADDRESS(ES) Air Force Office of Scientific Research 875 N. Randolph St., Rm. 3112 Arlington, VA 22203				10. SPONSOR/MONITOR'S ACRONYM(S)	
				11. SPONSOR/MONITOR'S REPORT NUMBER(S) AFRL-OSR-VA-TR-2013-0404	
12. DISTRIBUTION / AVAILABILITY STATEMENT DISTRIBUTION A: APPROVED FOR PUBLIC RELEASE					
13. SUPPLEMENTARY NOTES					
14. ABSTRACT An all-sky polarization spectral imager developed under prior support was deployed along with an atmospheric lidar, a sun-tracking multi-channel solar radiometer, and a variety of ground-based aerosol sensors to study the effect of variable aerosols, clouds, and surface reflectance on skylight polarization in the 450 - 780 nm spectral region. The entire sensor suite operated continuously from 2009-2012 except for brief periods of maintenance. This study produced a computer model for predicting clear-sky polarization as a function of aerosol properties and surface reflectance, which was validated with measurements and then used to predict clear-sky polarization spectra for various locations around the world. A surface reflectance with a strong wavelength dependence results in lower skylight degree of polarization at wavelengths with higher surface reflectance. Similarly, changing aerosol types and concentrations lead to spatially and temporally variable skylight polarization.					
15. SUBJECT TERMS Atmospheric polarization, polarimetric imaging, remote sensing, atmospheric propagation					
16. SECURITY CLASSIFICATION OF:			17. LIMITATION OF ABSTRACT	18. NUMBER OF PAGES	19a. NAME OF RESPONSIBLE PERSON
a. REPORT	b. ABSTRACT	c. THIS PAGE			19b. TELEPHONE NUMBER (include area code)

Final Report: Atmospheric Polarization Imaging with Variable Aerosols, Clouds, and Surface Albedo

Dr. Joseph A. Shaw (jshaw@montana.edu), Montana State University – Bozeman

Executive Summary

Effective prediction and exploitation of polarization signatures in optical remote sensing requires improved understanding of the underlying physical mechanisms and phenomenology. To this end we have developed and deployed an all-sky polarization imager, along with a wide range of atmospheric sensors, to study the influence of aerosols and clouds on skylight polarization in the visible and near-infrared spectral bands. We developed the all-sky polarization imager with prior AFOSR support, and this report focuses on its deployment and on some of its primary results.

Key results include the following:

- The cblah blah ...
-

This effort (April 2010 – April 2013) involved seven researchers:

1. Dr. Joseph A. Shaw – Professor and principal Investigator;
2. Dr. Nathan J. Pust – postdoctoral associate;
3. Mr. Andrew Dahlberg – graduate student working primarily on Mauna Loa polarization;
4. Mr. Michael Thomas – graduate student developing aerosol measurement capabilities in support of all-sky polarization imaging;
5. Mr. Paul Nugent – Research Engineer (supported primarily with NASA funding, but partly supported by AFOSR polarization funds);
6. Mr. Gavin Lommatsch – undergraduate student developing NIR polarimetry;
7. Ms. Elizabeth Forbes – undergraduate student studying wildfire smoke effect on skylight polarization.

Two graduate students successfully defended theses based fully on work supported by this grant:

1. Mr. Andrew Dahlberg – *All-sky polarization imager deployment at Mauna Loa Observatory, Hawaii* – M.S. Thesis, May 2010 (<http://etd.lib.montana.edu/etd/view/item.php?id=1048>).
Mr. Dahlberg continued Ph.D. studies with support under this grant, but his degree completion was delayed by emergency medical treatment in 2012.
2. Mr. Michael Thomas – *In-situ and solar radiometer measurements of atmospheric aerosols in Bozeman, Montana* – M.S. Thesis, December 2011. <http://scholarworks.montana.edu/xmlui/handle/1/2419>

The following **journal papers** were generated with full or partial support from this project:

1. K. S. Repasky, J. A. Reagan, A. R. Nehr, D. S. Hoffman, M. J. Thomas, J. L. Carlsten, J. A. Shaw, and G. E. Shaw, “Observational studies of atmospheric aerosols over Bozeman, Montana using a two color lidar, a water vapor DIAL, a solar radiometer, and

- a ground based nephelometer over a twenty four hour period,” J. Atmos. Ocean Technol. 28(3), 320-336, doi:10.1175/2010JTECHA1463.1 (Mar. 2011).
2. N. J. Pust and J. A. Shaw, “Comparison of skylight polarization measurements and MODTRAN-P calculations,” J. Appl. Rem. Sens. 5, 053529-1-053529-16, doi:10.1117/1.3595686 (2 June 2011).
 3. A. R. Dahlberg, N. J. Pust, and J. A. Shaw, “Skylight polarization measurements at Mauna Loa, Hawaii,” Opt. Express 19(17), 16008-16021, doi:10.1364/OE.19.016008, <http://www.opticsinfobase.org/oe/abstract.cfm?uri=oe-19-17-16008> (2011).
 4. J. A. Shaw, N. J. Pust, “Icy wave-cloud corona and cirrus iridescence,” Appl. Opt. 50(28), F6-F11, doi:10.1364/AO.50.0000F6 (2011).
 5. N. J. Pust, A. R. Dahlberg, M. J. Thomas, J. A. Shaw, “Comparison of full-sky polarization and radiance observations to radiative transfer simulations which employ AERONET products,” Opt. Express 19(19), 18602-18613, doi:10.1364/OE.19.018602 (2011).
 6. N. J. Pust and J. A. Shaw, “Wavelength dependence of the degree of polarization in cloud-free skies: simulations of real environments,” Opt. Express 20(14), 15,559-15,568 (2012).
 7. J. H. Churnside, R. Marchbanks, J. H. Lee, J. A. Shaw, A. Weidemann, P. Donaghay, “Airborne lidar detection and characterization of internal waves in a shallow fjord,” J. Appl. Rem. Sens. 6(1), 063611, doi:10.1117/1.JRS.6.063611 (2012) [experimental comparisons of linear and circular polarization for measurements in turbid media].
 8. J. A. Shaw, “Radiometry and the Friis Transmission Equation,” Am. J. Physics 81(1), 33-37 (2013).

The following **conference papers** were published with full or partial support from this project:

1. J. A. Shaw, N. J. Pust, B. Staal, J. Johnson, A. Dahlberg, “Continuous outdoor operation of an all-sky polarization imager,” Proc. SPIE **7672** (*Polarization: Measurement, Analysis, and Remote Sensing IX*), 76720A-1-7, 7 April 2010 (doi:10.1117/12.851374).
2. A. Dahlberg, N. J. Pust, and J. A. Shaw, “All-sky imaging of visible-wavelength atmospheric polarization at Mauna Loa, Hawaii,” Proceedings of the International Geoscience and Remote Sensing Symposium (ISBN 978-1-4244-9566-5), 1683-1686, 25 July 2010.
3. K. S. Repasky, A. R. Nehrir, D. S. Hoffman, M. J. Thomas, J. L. Carlsten, J. A. Shaw, “Observational studies of atmospheric aerosols in the lower troposphere using multiple sensors,” Proceedings of the International Geoscience and Remote Sensing Symposium (ISBN 978-1-4244-9566-5), 2583-2586, 25 July 2010.
4. J. A. Shaw, “Observing light in nature from an airplane window,” Proc. SPIE **7782** (*The Nature of Light: Light in Nature III*), 2 Aug. 2010.
5. N. J. Pust, A. R. Dahlberg, and J. A. Shaw, “Comparison of sky polarization observations to radiative transfer simulations which use AERONET retrieval data,” Proc. SPIE **8160** (*Polarization Science and Remote Sensing V*), 81600G, doi:10.1117/12.894637, 21-22 Aug. 2011.

6. J. A. Shaw and N. J. Pust, "Dual-polarization lidar identification of ice in a corona-producing wave cloud," *Proc. SPIE* **8160**, 81600I, doi:10.1117/12.894893, 21-22 Aug. 2011.
7. J. H. Churnside, R. D. Marchbanks, J. H. Lee, J. A. Shaw, A. Weidemann, P. L. Donaghay, "Airborne lidar sensing of internal waves in a shallow fjord," **invited paper**, *Proc. SPIE* **8372** (*Ocean Sensing and Monitoring IV*), 83720P, doi: 10.1117/12.918099, 2012.

The following **conference presentations** were given (without published paper) with partial or full support from this project:

1. J. A. Shaw and N. J. Pust, "Lunar corona in ice wave cloud," 10th International Meeting on Light and Color in Nature, St. Mary's College of Maryland, 16-20 June 2010.
2. N. Kaufman, B. Staal, J. A. Shaw, P. W. Nugent, N. J. Pust, D. Mikes, C. Knierim, R. Torgerson, R. Larimer, "Optical sensors for education and outreach," Optical Technology Center (OpTeC) annual meeting, Montana State University, Bozeman, MT, 26 Aug. 2010.
3. A. R. Dahlberg, N. J. Pust, J. A. Shaw, "All-sky imaging of visible-wavelength atmospheric polarization at Mauna Loa, Hawaii," Optical Technology Center (OpTeC) annual meeting, Montana State University, Bozeman, MT, 26 Aug. 2010.
4. N. J. Pust, A. R. Dahlberg, J. A. Shaw, "Full-sky radiance models," Optical Technology Center (OpTeC) annual meeting, Montana State University, Bozeman, MT, 26 Aug. 2010.
5. M. Thomas, J. A. Shaw, N. J. Pust, G. E. Shaw, K. S. Repasky, J. A. Reagan, "In-situ and solar radiometer measurements of aerosols over MSU," Optical Technology Center (OpTeC) annual meeting, Montana State University, Bozeman, MT, 26 Aug. 2010.
6. J. A. Shaw, "Optics in Nature," Keynote Speech, International OSA Network of Students Conference – North America (IONS2-NA), College of Optical Sciences, University of Arizona, Tucson, AZ, 1 Oct. 2010.
7. J. A. Shaw, N. J. Pust, A. R. Dahlberg, "All-sky polarization imaging," Invited talk at MISR User's Workshop, California Institute of Technology, Pasadena, CA, 9-10 Dec. 2010.
8. M. J. Thomas, T. L. Lathem, J. A. Shaw, G. E. Shaw, A. Nenes, N. J. Pust, K. S. Repasky, "Aerosols in clean and smoky air at Bozeman, Montana," American Geophysical Union (AGU) Fall Meeting, San Francisco, CA, 13-17 Dec. 2010.
9. N. J. Pust, J. A. Shaw, A. R. Dahlberg, "Comparison of observed full-sky polarization to radiative transfer model using AERONET retrieval inputs," American Geophysical Union (AGU) Fall Meeting, San Francisco, CA, 13-17 Dec. 2010.
10. N. J. Pust, A. R. Dahlberg, and J. A. Shaw, "All-sky polarization measurements and comparisons to MODTRAN-P and other radiative transfer codes," 33rd Review of Atmospheric Transmission Models (2011 IEEE Transmission Meeting), Lexington, MA, 14-16 June, 2011.
11. A. R. Dahlberg, N. J. Pust, and J. A. Shaw, "Effect of surface reflectance on sky polarization at Mauna Loa, Hawaii," Optical Technology Center (OpTeC) annual meeting, Montana State University, Bozeman, MT, 18 Aug. 2011.

12. J. A. Shaw, N. J. Pust, A. Dahlberg, "Full-sky atmospheric polarization imaging," Air Force Office of Scientific Research 2012 Remote Sensing and Imaging Program Review, Albuquerque, NM, 29 March 2012.
13. N. J. Pust and J. A. Shaw, "Full-sky atmospheric polarization imaging in the visible/NIR," Workshop on concepts in electromagnetic scattering for particulate-systems characterization, Memphis, TN, 17-19 May 2012.
14. J. A. Shaw, P. W. Nugent, J. Johnson, "Radiometric infrared imaging with compact microbolometer cameras: from clouds to beehives," **Invited talk** at *Infrared: science, technology, and applications*, 506th Wilhelm and Else Heraeus-Seminar, Bad Honnef, Germany, 21-23 May 2012.
15. T. L. Lathem, B. E. Anderson, A. J. Beyersdorf, L. Thornhill, E. Winstead, J. A. Shaw, M. J. Thomas, G. E. Shaw, A. Nenes, "Cloud condensation nuclei activity and hygroscopicity of in-situ biomass burning aerosol," American Assoc. Aerosol Research 31st Annual Conference, Minneapolis, MN, Oct. 8-12, 2012.
16. E. Forbes, J. A. Shaw, N. J. Pust, "Effects of wildfire smoke on the optical polarization of skylight," Student Research Celebration, Montana State University, Bozeman, MT, 18 April 2013.
17. G. Lommatsch, J. A. Shaw, N. J. Pust, "Characterizing light polarization in the near infrared," Student Research Celebration, Montana State University, Bozeman, MT, 18 April 2013.

The following **conferences** were chaired and special journal issues edited by the P.I. with support from this grant:

1. K. Creath and J. A. Shaw, eds., *The nature of light: light in nature III*, SPIE Proceedings **7782**, 2010.
2. J. A. Shaw and J. S. Tyo, eds., *Polarization Science and Remote Sensing V*, SPIE Proceedings **8160**, 9 Sep. 2011.
3. J. A. Shaw, R. L. Lee, Jr., and P. L. Marston, eds., feature issue of Applied Optics on Light and color in the open air, *Applied Optics* **50**(328), 1 Oct. 2011.
4. Light and color in the open air conference, University of Alaska – Fairbanks, Aug. 2013.
5. J. A. Shaw and D. L. LeMaster, *Polarization Science and Remote Sensing VI*, SPIE, San Diego, CA, Aug. 2013.

The following **book chapter** was published with support from this grant:

1. J. S. Tyo, D. B. Chenault, J. A. Shaw, D. H. Goldstein, "Techniques in Imaging Polarimetry," Chapter 18 in D. H. Goldstein, *Polarized Light*, 3rd ed., pp. 377-400, CRC Press (Boca Raton, FL), 2011.

Introduction

Optical polarization increasingly is being used to gain information beyond that offered by spectral, spatial, and intensity variations in images for detecting and identifying man-made objects in space, in the air, or on the ground (Tyo et al. 2006). This often involves imaging or sensing through the atmosphere, in which case there is an urgent need to understand the naturally occurring polarized light in the atmosphere and how the atmosphere modifies polarized light as it travels along an open-air propagation path.

The clear sky has a distinct pattern of partially polarized light that peaks in a band stretching across the sky 90° from the Sun. Rayleigh scattering theory predicts that the degree of linear polarization (DoLP) in this band of maximum polarization will significantly exceed 90%, but in the real atmosphere multiple scattering reduces the maximum value to between 80 and 90% (Coulson 1988). Aerosols and cloud particles, which are comparable to or larger than the optical wavelength, alter the pure Rayleigh background through scattering processes that do not follow the simple Rayleigh law. Consequently, predicting the polarization pattern observed in the real atmosphere, under conditions other than those leading to pristine Rayleigh scattering, requires careful treatment of the scattering of light by aerosols and cloud particles (Pust and Shaw 2006, 2007, 2008, 2009, 2011, 2012; Pust et al. 2008, 2009a, 2009b, 2011; Shaw 2007; Shaw et al. 2010). Furthermore, light reflected from the ground mixes with the polarized skylight, generally reducing the net degree of polarization (DoP) observed in the atmosphere (Dahlberg et al. 2011).

In this effort we used an all-sky polarization imaging system that we developed with earlier Air Force research funding (Pust and Shaw 2006; Pust and Shaw 2008) to record carefully calibrated all-sky images of vis-NIR polarization from the ground (Shaw et al. 2010), and we used data from that system and supporting meteorological sensors to develop a model of clear-sky polarization (Pust and Shaw 2012; Pust et al. 2011). This model is built around a Successive Orders of Scattering (SOS) radiative transfer code (LeNoble et al. 2007) provided us by the NASA AERONET program (Holben 1998). It incorporates measurements of aerosol physical and optical properties and ground reflectance to create accurate simulations of all-sky polarization patterns that we have validated with measured all-sky polarization images (Pust et

al. 2011). Because this model includes scattering calculations based on measured aerosol parameters, it exceeds the capabilities of the early MODTRAN-P polarized radiative transfer code version that we used in an earlier comparison (Pust & Shaw 2009).

This project produced measurement capabilities, measurement results, and simulation results that greatly enhance our understanding of polarized light scattering in the atmosphere, including the effects of clouds, aerosols, and the underlying surface. Quantifying these effects provides crucial information for the practical use of polarization imaging by the Air Force. The polarization state of skylight and atmospheric modification of polarized light are important for polarimetric object detection or identification because they determine the illuminating conditions for the scene. Under some conditions, an object's polarization signature can even disappear entirely. For example, this has been shown to occur for thermal infrared signatures when the p-polarized emission is comparable to the s-polarized reflection term (Felton et al. 2010; Fetrow et al. 2000; Gurton et al. 2008, 2010; Shaw 1999, 2002; Tyo et al. 2007), but it also will occur at visible and near-infrared wavelengths if the initial skylight polarization compensated for the polarization that occurs on reflection from the object (Pust et al. 2008, 2009).

2. The Atmospheric Polarization Imager (API) System

In previous research we designed, built, and calibrated an all-sky polarization imager (API) instrument (Pust and Shaw 2009), and deployed it outdoors continuously since 2009 (Shaw et al. 2010). This instrument expands the capabilities of previous all-sky polarization imagers to enable the first quantitative studies of sky polarization in partly cloudy skies. For example, it provides real-time digital data and removes the uncertainty of film processing inherent in systems described by North and Duggin (1997) and Horvath et al. (2002). Our use of electronically tunable liquid crystal variable retarders (LCVRs) allows the API to achieve much faster Stokes-image acquisition than instruments that rely on rotating polarization elements (Cronin et al. 2006; Voss and Liu 1997; Kreuter et al. 2009), enabling operation in changing aerosol and cloud conditions without polarization artifacts. The API instrument records a Stokes vector at each pixel of a 1-Mpixel image of the full sky dome in approximately 0.3, depending on the required exposure time (Pust and Shaw 2006). The four elements of the Stokes vector, or Stokes parameters, completely describe the polarization state of the light detected at each pixel.

These parameters are used to calculate the DoLP, which expresses the percentage of the incident light that is polarized, and the AoP, which expresses the orientation of the polarized light.

The API system achieves rapid polarimetric tuning through the use of LCVRs and a fixed linear polarizer, but relies on a rotating filter wheel for the slower spectral tuning that can be accepted in these studies. The system can be used with a fisheye front-end optics module for all-sky imaging, or a telephoto module for remote target polarization signature imaging. The all-sky version has been used also to simultaneously measure the polarization signature of ground-based objects and the changing overhead sky polarization pattern (Pust et al. 2009).

Figure 1 is an optical layout diagram photograph of the API system. The front-end optical module at the left is followed by two field lenses that direct wide-angle light into the polarimeter to the right. The polarimeter contains two liquid crystal variable retarders (LCVRs), a fixed linear polarizer, a 10-nm spectral filter in a rotation stage, and a Nikon 105-mm micro lens that reduces the image to the size of the 1-megapixel CCD. The two LCVRs are electronically tuned to four different retardance states determined with optimization techniques described by Sabatke et al. (2000) and Tyo (2000; 2002). An image is recorded at each retardance state and the set of four images is used to retrieve a system matrix that allows calculation of Stokes vectors at each pixel (Pust and Shaw 2006). The instrument can record a full 1-MPixel Stokes image of the entire daytime sky in 0.3 s at a single wavelength with DoP uncertainty less than 2% (and usually much better), depending on incident polarization state. A key capability of this system is imaging an all-sky Stokes image rapidly enough to avoid polarization artifacts that otherwise would arise from cloud motion. Whereas the API obtains data rapidly at multiple polarization states, it relies on a slower rotating filter wheel to select one of five wavelength channels defined by 10-nm-wide filters (currently at 450, 490, 530, 670, and 780 nm, but easily changed).

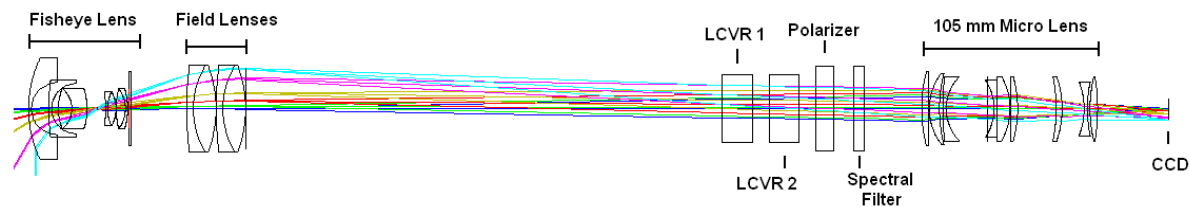


Figure 1. Layout of the Atmospheric Polarization Imager (API) system with fisheye optics.

Figure 2 is a photograph of the API system deployed in a white weather-proof housing on a rooftop platform. It operated nearly continuously in that position from late 2009 to fall 2012, providing an unprecedented data set that allows atmospheric polarization to be studied as a function of many environmental parameters under widely varying conditions (in fall 2012 operated was temporarily suspended for the camera to be upgraded). The instrument mounted on the left-hand corner of the platform is a sun-sky scanning radiometer, which measures direct solar irradiance and sky radiance in eight spectral bands spread between 340 nm and 1640 nm. This instrument is part of the world-wide NASA AERONET network (Holben et al. 1998), from which we obtain retrieved values of aerosol optical properties such as optical depth, particle size distributions, and complex refractive index when the sun is directly visible.



Figure 2. All-sky polarization imager system mounted in white weather-proof housing with automated sun occulter (right) and multi-wavelength solar radiometer (left) mounted on rooftop platform for continuous daytime measurements at Montana State University in Bozeman, Montana.

3. Atmospheric Polarization Measurements with a Clear Sky

Examples of all-sky images from the API are shown in Figure 3 in mostly clear-sky conditions. The left-hand image is the DoLP, and the right-hand image is the AoP. The band just below the center of each image is the sun occulter that prevents the imager from viewing the sun directly. Thousands of such images have been recorded while the API system has been deployed

outdoors nearly continuously since late 2009. This large and varied data base has allowed us to develop and refine new understanding of how the polarization varies with aerosols and surface reflectance, and to a lesser degree, with clouds. During the most recent funding, we progressed to the point that we understand and can predict clear-sky, daytime sky polarization in the Vis-NIR spectral range with quantitative accuracy of a few % or better, as detailed in the following subsections.

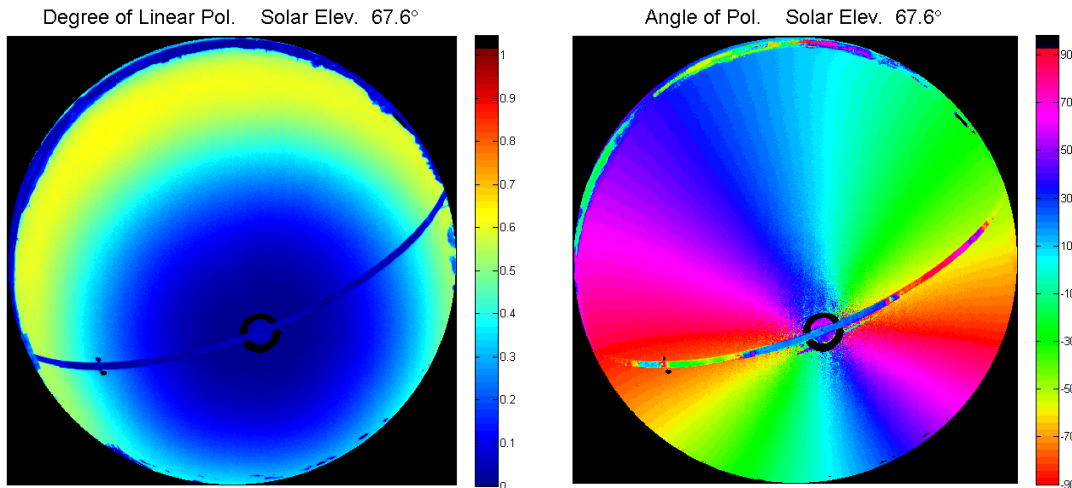


Fig. 3. All-sky images of DoLP (left) and AoP (right) for a clear sky in the early afternoon with clean air (500-nm atmospheric optical depth = 0.19) at 700 nm. The band across each image is the sun occulter.

4. Comparison of Measurements with MODTRAN-P Simulations

One of our original goals in developing the all-sky polarization imager was to provide validation data for validating the polarized radiative transfer code, MODTRAN-P, developed at the Air Force Research Laboratory (AFRL). The comparisons showed that the MODTRAN-P code produces reasonable results in very clean-sky conditions (low aerosol content), particularly at long visible wavelengths (Pust and Shaw 2009, 2011). However, with higher aerosol optical depth, the single-scattering version of MODTRAN-P overestimated the degree of polarization, particularly at shorter wavelengths (less than about 630 nm). This comparison highlighted the need for including properly implemented multiple scattering in any code that is used to predict atmospheric polarization. It also emphasized the need for well-characterized aerosol properties. The details of this comparison were included in our previous report, and they were published in the peer-reviewed literature during this funding cycle (Pust & Shaw 2011). It should be noted

also that we recently obtained a copy of the latest version of MODTRAN-P, which does include a multiple-scattering model, but we have not yet had a chance to fully analyze its capabilities.

5. Effect of Surface Reflectance on Clear-Sky Polarization

In 2008 we deployed our atmospheric polarization imager to the Mauna Loa Observatory (MLO) on the island of Hawaii to measure clear-sky polarization under the cleanest possible conditions that approach pure Rayleigh scattering. This location provided another extremely valuable characteristic, which is a frequently changing surface reflectance. Whereas the volcanic mountain itself is a very dark surface, it is common for clouds to develop at lower elevations and slowly climb up toward the observatory. The result is a continually changing surface reflectance beneath a clear sky, as shown in the photograph of Figure 4. The continual and rapid change in underlying reflectance allowed us to more quickly and effectively study the influence of surface reflectance on the observed skylight polarization.

We used satellite imagery to determine the effective surface reflectance for the area surrounding the MLO, and processed clear-sky measurements from the two-week experiment to obtain the curve shown in Figure 5. This curve shows how the maximum clear-sky polarization values became lower as the amount of upwelling radiance from the surface increased. In other words, it indicates the pattern with which the maximum clear-sky DoLP was reduced by increasing reflectance of the underlying surface (Dahlberg et al. 2011). The regression shown in Figure 5 tells us that we can estimate the clear-sky DoLP at a wavelength of 450 nm as $0.54 - 0.184\rho + 0.26\exp(-0.006L)$, where ρ is an isotropic surface albedo (i.e., reflectance), and L is the upwelling radiance from the surface. Similar regressions at other wavelengths are available in the literature (Dahlberg et al. 2011). This study made it clear that any quantitative analysis or prediction of skylight polarization must also include careful consideration of the underlying surface reflectance. In a future section of this report, we show that a strong wavelength variation of surface reflectance also can produce dramatic changes in the polarization of skylight (Pust and Shaw 2012).



Figure 4. Atmospheric Polarization Imager deployed in front of a telescope dome, surrounded by black lava rock at the Mauna Loa Observatory on the island of Hawaii. In this photo, clouds have developed to fill the “saddle” region between Mauna Loa and Mauna Kea in the background (home of the Keck and other astronomical telescopes). The frequently changing clouds provided a wide variation in effective surface reflectance below the clear overhead sky. The mechanism for this effect is the mixing of largely unpolarized light reflected from the surface with the otherwise highly polarized light scattered by the atmosphere, resulting in a net reduction of skylight polarization.

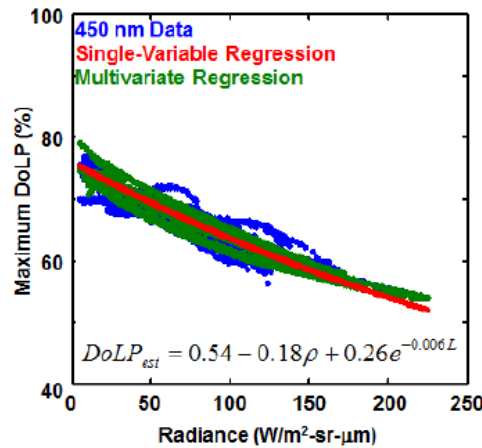


Figure 5. Regression of the maximum degree of linear polarization (DoLP) at 450 nm wavelength with upwelling radiance observed by the GOES satellite in the vicinity of the Mauna Loa Observatory during our June 2008 deployment. This shows that the clear-sky maximum DoLP varied from 50% to 80% in a manner predictable by the changing surface reflectance. The regression equation includes the measured degree of linear polarization (DoLP), isotropic surface albedo (ρ), and upwelling radiance from the surface (L).

6. Development of Clear-Sky Polarization Model

During this project, one of our primary objectives was to develop a computer model for predicting clear-sky polarization under realistic conditions. We accomplished this by developing a Matlab program that reads in surface reflectance from satellite images and aerosol parameters from an AERONET solar radiometer and other ground-based aerosol sensors, and uses an SOS radiative transfer code (LeNoble 2007) to perform multiple-scattering calculation to predict the clear-sky polarization that would be observed with the measured aerosol and surface parameters. By running the model for a large number of angles, we can generate simulated all-sky polarization images and thereby compare directly to our observations. These comparisons have shown that we can very reliably and accurately predict the observations, as long as we have access to reliable aerosol and surface-reflectance data (Pust et al. 2011). An example comparison is shown in Figure 6. The left-hand column in this figure is the measured all-sky image of radiance (top) and DoLP (bottom). The center column is the simulated all-sky image of radiance (top) and DoLP (bottom) (the simulated images do not include the sun occulter). The right-hand column is the difference of measured minus simulated values (radiance on top, DoLP on bottom). It is encouraging that the DoLP differences are within 2% over most of the image.

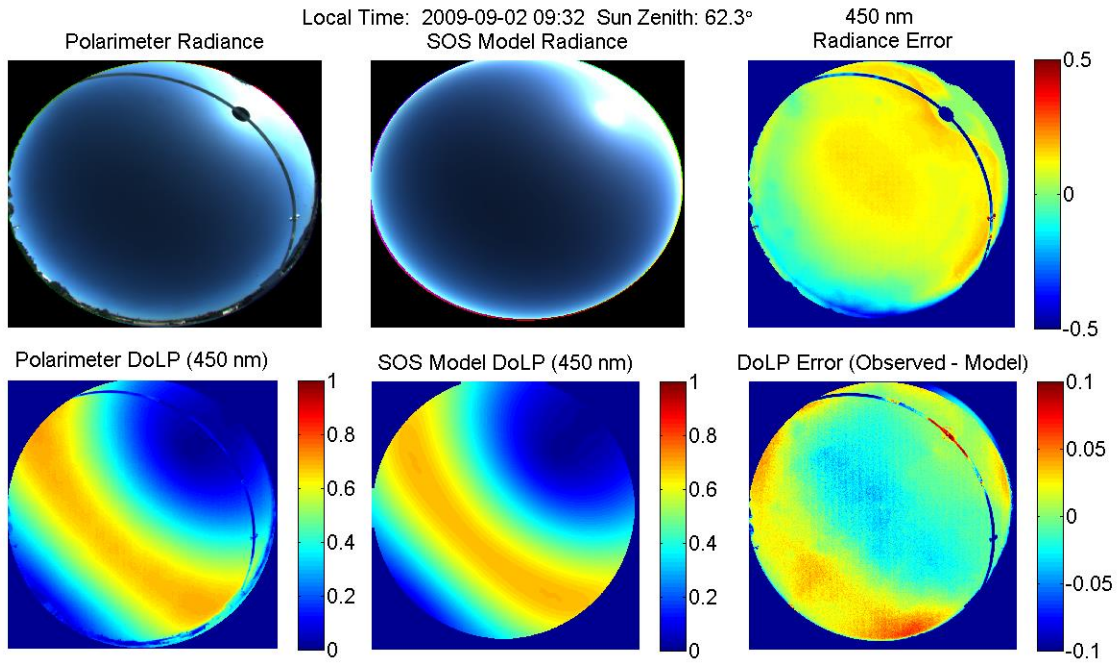


Figure 6. Measured (left) and simulated (center) all-sky images of radiance (top) and DoLP (bottom). The right-hand column shows difference images of measured – simulated.

7. Combined Measurements and Simulations for Predicting Polarization Spectra

Our first application of the validated clear-sky polarization model was to use it with measured aerosol parameters and surface reflectance to study Vis-NIR polarization spectra that would be observed under the measured aerosol and surface conditions in various locations around the world. The primary question we were addressing in this study was whether or not there was a simple way of predicting the spectral distribution of skylight polarization. By using aerosol data from AERONET stations around the world, along with coincident satellite measurements of surface reflectance, we were able to determine that the answer to this question is “no – there is no simple way of predicting the expected skylight polarization without knowing aerosol and surface parameters.” Said another way, there is no simple spectrum of skylight polarization. In fact, the actual Vis-NIR spectrum of skylight polarization can increase or decrease with wavelength, and can do so in very interesting manners when the underlying surface has a spectrally varying reflectance (Pust & Shaw 2012).

The broad diversity of wavelength variation in skylight is illustrated in Figure 7, which shows three spectra of simulated maximum skylight DoLP (simulations based on measured aerosol parameters and surface reflectance spectra). The top curve is a calculation based on aerosol and surface measurements at Barrow, Alaska with a very clean atmosphere that provides nearly Rayleigh-scattering conditions (aerosol optical depth = $AOD = 0.02$). The underlying surface was tundra observed in September, so it has a very low and spectrally flat reflectance. The result was a spectrum that very nearly approached the polarization expected for an ideal Rayleigh scattering atmosphere (Pust and Shaw 2006; Coulson 1988). The middle curve was a calculation based on aerosol and surface reflectance measurements at Ames, Iowa, with modest aerosols ($AOD = 0.08$) and a mid-summer green vegetation-covered surface. This was a particularly interesting case because the polarization spectra included a rapid drop of polarization at 700 nm, caused by a rapid increase of vegetation reflectance in the NIR. The bottom curve was based on measurements at Saada, Morocco, with high aerosol content ($AOD = 0.3$) and a desert surface with relatively high and spectrally flat reflectance.

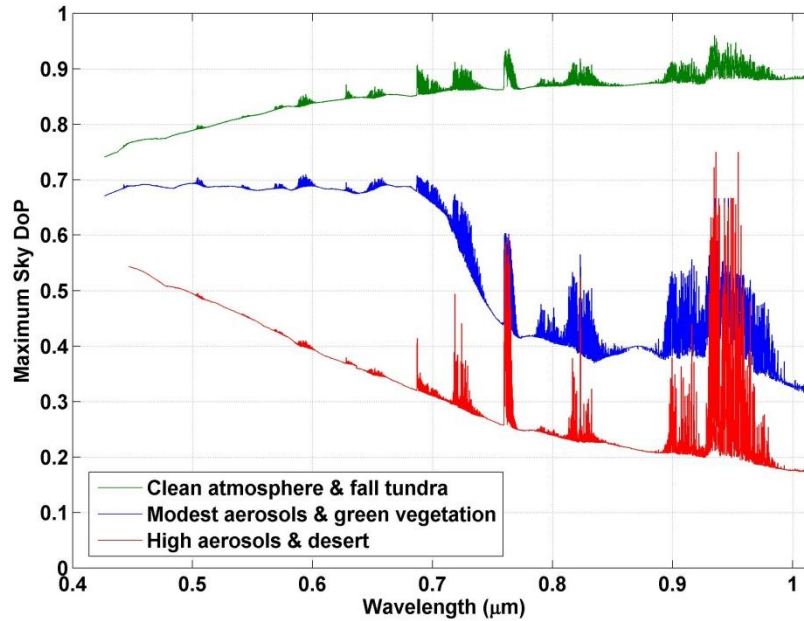


Figure 7. Vis-NIR spectra of the maximum degree of polarization expected for measured aerosol and surface-reflectance parameters for: (top) Barrow, Alaska with aerosol optical depth = AOD = 0.02 and a dark, spectrally flat tundra surface; (middle) Ames, Iowa with AOD = 0.08 and a surface covered with green vegetation whose reflectance increases strongly at wavelengths past 700 nm; and (bottom) Saada, Morocco with AOD = 0.3 and a desert surface with relatively bright but spectrally flat desert surface.

Effect of Wildfire Smoke Aerosol on Skylight Polarization

As this grant came to a close, we were in the midst of studying the effect of wildfire smoke aerosol on the polarization observed in a cloud-free sky. This study focused on measurements obtained on and near August 28, 2012, at Montana State University in Bozeman, Montana. Late on the afternoon of August 28, a relatively smoke-free atmosphere became contaminated on the south side by a smoke plume rising from a newly burning wildfire. Figure 8 is a wide-angle photograph of the plume rising from the mountains to the south and extending across the eastern side of Bozeman. Figures 9-11 are all-sky polarization images recorded with our instrument at Montana State University, along with profiles through the band of maximum DoLP in each image. This image sequence shows clearly that a quite symmetric pattern of clear-sky polarization rapidly changed to become very asymmetric. The maximum DoLP also fell substantially – from approximately 0.69 before the smoke plume on August 28 (Figure 9) to less than 0.3 within the thick smoke plume on August 29 (Figure 11). Figure 12 shows a time-series plot of aerosol scattering and extinction coefficients measured with our aerosol sensors. For

reference, these parameters are often in the range of 10 Mm^{-1} when the very clean Montana sky is devoid of wildfire smoke, and are typically in the range of $30\text{-}60 \text{ Mm}^{-1}$ in large cities with substantial urban pollution. The values shown here, which briefly exceed 400 Mm^{-1} , are extreme values found in this region only during episodes of intense wildfire smoke. Detailed analysis of the aerosols in this smoke plume and their effect on the skylight polarization will be reported in the literature with a paper in preparation (Shaw et al. 2013).



Figure 8. Wide-angle photograph of a smoke plume rising from the mountains south of Bozeman, Montana (right-hand side) and traveling toward the east (left-hand side) on August 28, 2012.

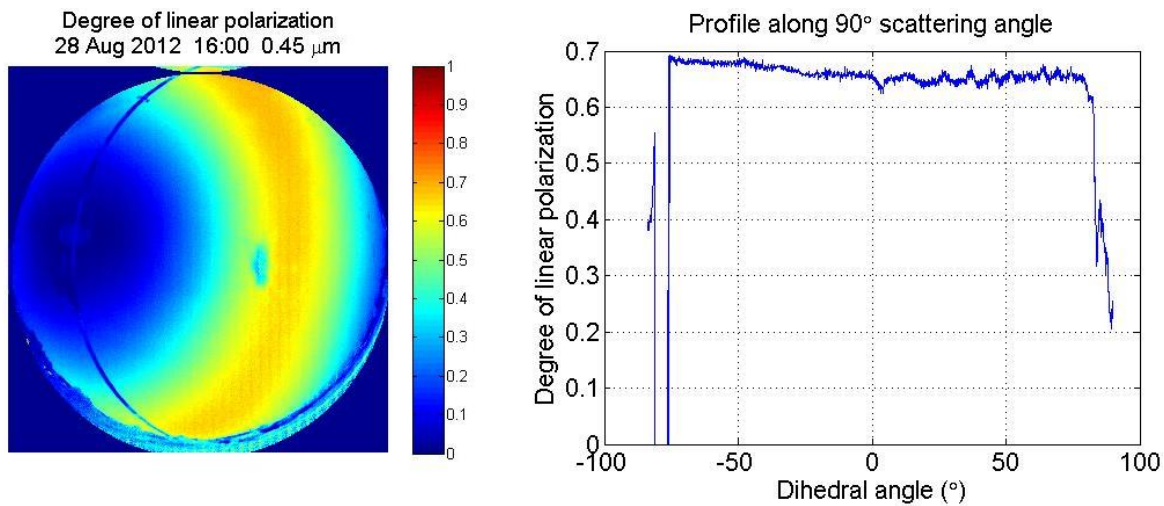


Figure 9. All-sky image of skylight degree of polarization (left) and profile through the band of maximum polarization (right) at 1600 Mountain Daylight Time on August 28, 2012, before the smoke plume arose.

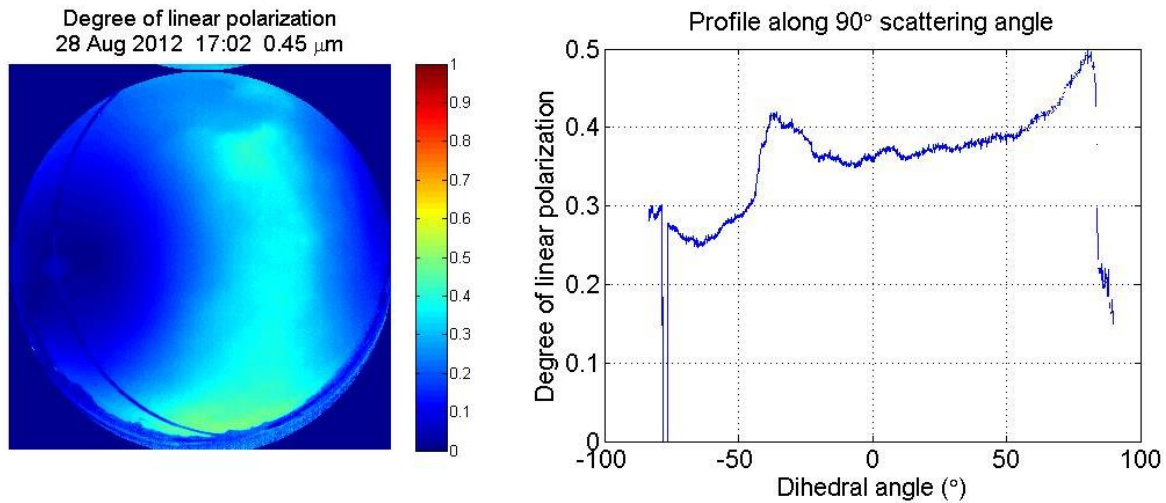


Figure 10. All-sky image of skylight degree of polarization (left) and profile through the band of maximum polarization (right) at 1702 Mountain Daylight Time on August 28, 2012, as the smoke plume was rising to the south (top of the all-sky image).

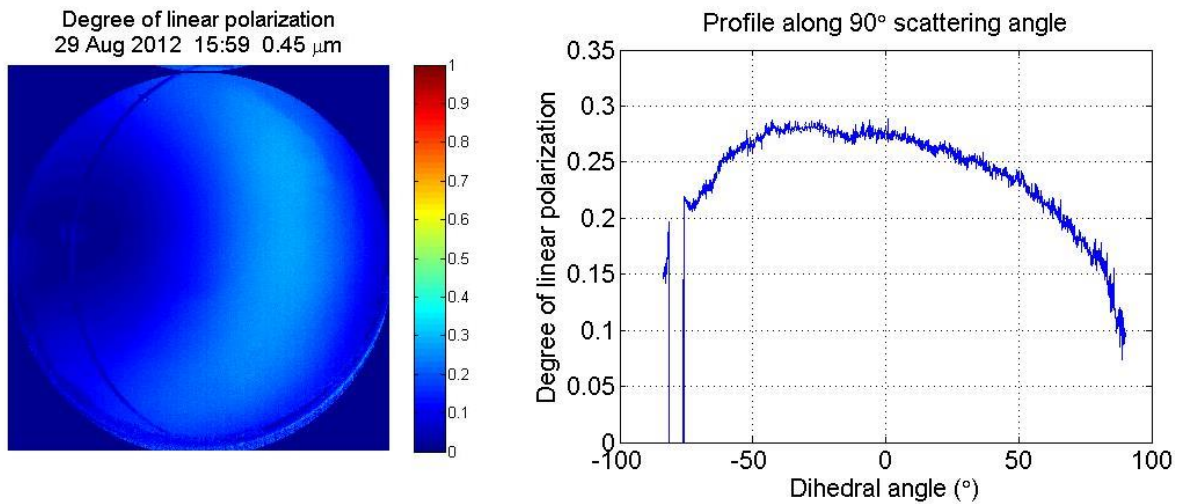


Figure 11. All-sky image of skylight degree of polarization (left) and profile through the band of maximum polarization (right) at 1559 Mountain Daylight Time on August 29, 2012, after the plume had filled the valley with smoke.

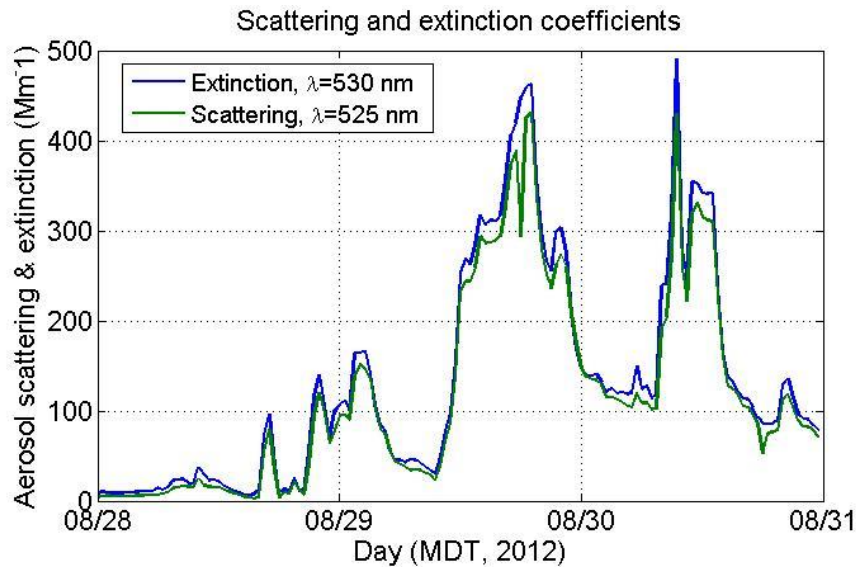


Figure 12. Time-series plot of aerosol extinction and scattering coefficients (the difference represents aerosol absorption) for August 28-30, 2012, as the sky went from relatively clean conditions to variably smoky.

References

- Cronin, T. W., E. J. Warrant, and B. Greiner, "Celestial polarization patterns during twilight," *Appl. Opt.* **45**(22), 5582-5589 (2006).
- Dahlberg, A. R., N. J. Pust, and J. A. Shaw, "Effects of surface reflectance on skylight polarization measurements at the Mauna Loa Observatory," *Optics Express* **19**(17), 16008-16021 (2011).
- Felton, M., K. P. Gurton, J. L. Pezzaniti, D. B. Chenault, and L. E. Roth, "Measured comparison of the crossover periods for mid- and long-wave IR (MWIR and LWIR) polarimetric and conventional thermal imagery," *Optics Express* **18**(15), 15704-15713 (2010).
- Fetrow, M. P., S. H. Sposato, K. P. Bishop, and T. R. Caudill, "Spectral polarization signatures of materials in the LWIR," *Proc. SPIE* **4133**, 249-260 (2000).
- Gurton, K. P., and M. Felton, "Variation in MidIR and LWIR polarimetric imagery due to diurnal and meteorological effects," *SPIE Proc.* **6972**, 69720W (2008).
- Gurton, K., M. Felton, R. Mack, D. LeMaster, C. Farlow, M. Kudenov, and L. Pezzaniti, "MidIR and LWIR polarimetric sensor comparison study," *SPIE Proc.* **7672**, 767205 (2010).
- Holben, B. N., T. F. Eck, I. Slutsker, D. Tanre, J. P. Buis, A. Setzer, E. Vermote, J. A. Reagan, Y. J. Kaufman, T. Nakajima, F. Lavenue, I. Jankowiak, and A. Smirnov, "AERONET – a federated instrument network and data archive for aerosol characterization," *Remote Sens. Env.* **66**(1), 1-16 (1998).

- Horvath, G., A. Barta, J. Gal, B. Suhai, and O. Haiman, "Ground-based full-sky imaging polarimetry of rapidly skies and its use for polarimetric cloud detection," *Appl. Opt.* **41**(3), 543-559 (2002).
- Kreuter, A., M. Zangerl, M. Schwarzmann, and M. Blumthaler, "All-sky imaging: a simple, versatile system for atmospheric research," *Appl. Opt.* **48**(9), 1091-1097 (2009).
- Lenoble, J., M. Herman, J. L. Deuzé, B. Lafrance, R. Santer, and D. Tanré, "A successive order of scattering code for solving the vector equation of transfer in the earth's atmosphere with aerosols," *J. Quant. Spect. Rad. Trans.* **107**(3), 479-507 (2007).
- North, J. and M. Duggin, "Stokes vector imaging of the polarized sky-dome," *Appl. Opt.* **36**(3), 723-730 (1997).
- Pust, N. J. and J. A. Shaw, "Dual-field imaging polarimeter using liquid crystal variable retarders," *Appl. Opt.* **45**(22), 5470-5478 (2006).
- Pust, N. J. and J. A. Shaw, "All-sky polarization imaging," *SPIE Proc.* **6682**, 668204 (2007).
- Pust, N. J. and J. A. Shaw, "Digital all-sky polarization imaging of partly cloudy skies," *Appl. Opt.* **47**(34), H190-H198 (2008).
- Pust, N. J., J. A. Shaw, and A. R. Dahlberg, "Visible-NIR imaging polarimetry of metal surfaces viewed under a variable atmosphere," *Proc. SPIE 6972 (Polarization: Measurement, Analysis, and Remote Sensing VIII)*, Orlando, FL), 18-19 Mar. (2008).
- Pust, N. J., A. Dahlberg, J. A. Shaw, "How good is a single-scattering atmospheric polarization model?," *Proc. SPIE 7461, (Polarization Science and Remote Sensing III)*, San Diego, CA), 3-4 Aug. (2009a).
- Pust, N. J., A. Dahlberg, J. A. Shaw, "Simultaneous measurements of polarization from metal plates and the sky," *Proc. SPIE 7461, (Polarization Science and Remote Sensing III)*, San Diego, CA), 3-4 Aug. (2009b).
- Pust, N. J. and J. A. Shaw, "Comparison of skylight polarization measurements and MODTRAN-P calculations," *J. Appl. Rem. Sens.* **5**, 053529 (2011).
- Pust, N. J., A. R. Dahlberg, M. J. Thomas, and J. A. Shaw, "Comparison of full-sky polarization and radiance observations to radiative transfer simulations which employ AERONET products," *Optics Express* **19**(19), 18602-18613 (2011).
- Pust, N. J. and J. A. Shaw, "Wavelength dependence of the degree of polarization in cloud-free skies: simulations of real environments," *Optics Express* **20**(14), 15559-15568 (2012).
- Sabatke, D. S., M. R. Descour, E. L. Dereniak, "Optimization of retardance for a complete Stokes polarimeter," *Optics Letters* **25**, 802-804 (2000).

Shaw, J. A., "Degree of linear polarization in spectral radiances from water-viewing infrared radiometers," *Appl. Opt.* **38**(15), 3157-3165 (1999).

Shaw, J. A., "The effect of instrument polarization sensitivity on sea surface remote sensing with infrared spectroradiometers," *J. Atm. Ocean. Technol.* **19**, 820-827 (2002).

Shaw, J. A., "A survey of infrared polarization in the outdoors," Proc. SPIE **6660** (Infrared Systems and Photoelectronic Technology II), DOI: 10.1117/12.741897 (2007).

Shaw, J. A., N. J. Pust, B. Staal, J. Johnson, A. Dahlberg, "Continuous outdoor operation of an all-sky polarization imager," Proc. SPIE **7672** (*Polarization: Measurement, Analysis, and Remote Sensing IX*), 76720A-1-7, 7, doi:10.1117/12.851374 (2010).

Shaw, J. A., N. J. Pust, and E. Forbes, "Asymmetric skylight polarization pattern caused by wildfire smoke aerosols," *Remote Sens.* (in press, July 2013).

Tyo, J. S., "Noise equalization in Stokes parameter images obtained by use of variable retardance polarimeters," *Optics Letters* **25**, 1198-2000 (2000).

Tyo, J. S., "Design of optimal polarimeters: maximum of signal-to-noise ratio and minimization of systematic error," *Appl. Opt.* **41**, 619-630 (2002).

Tyo, J. S., D. L. Goldstein, D. B. Chenault, and J. A. Shaw, "Review of passive imaging polarimetry for remote sensing applications," *Appl. Opt.* **45**(22), 5453-5469 (2006).

Tyo, J. S., B. M. Ratliff, J. K. Boger, W. T. Black, D. L. Bowers, and M. P. Fetrow, "The effects of thermal equilibrium and contrast in LWIR polarimetric images," *Optics Express* **15**(23), 15161-15167, doi:10.1364/OE.15.015161 (2007).

Voss, K. and Y. Liu, "Polarized radiance distribution measurements of skylight. I. system description and characterization," *Appl. Opt.* **36**(24), 6083-6094 (1997).